

# Structure and Bonding in Small Neutral Alkali-Halide Clusters

Andrés Aguado

*Departamento de Física Teórica, Facultad de Ciencias, Universidad de Valladolid, 47011 Valladolid, Spain*

Andrés Ayuela

*Institut für Theoretische Physik, Technische Universität Dresden, 01062 Dresden, Germany*

José M. López and Julio A. Alonso

*Departamento de Física Teórica, Facultad de Ciencias, Universidad de Valladolid, 47011 Valladolid, Spain*

(September 9, 1997)

The structural and bonding properties of small neutral alkali-halide clusters,  $(AX)_n$  with  $n \leq 10$ ,  $A = Li^+, Na^+, K^+, Rb^+$  and  $X = F^-, Cl^-, Br^-, I^-$ , are studied using the *ab initio* Perturbed Ion (PI) model and a restricted structural relaxation criterion. A trend of competition between rock-salt and hexagonal ring-like isomers is found and discussed in terms of the relative ionic sizes. The main conclusion is that an approximate value of  $r_C/r_A = 0.5$  (where  $r_C$  and  $r_A$  are the cationic and anionic radii) separates the hexagonal from the rock-salt structures. The classical electrostatic part of the total energy at the equilibrium geometry is enough to explain these trends. The magic numbers in the size range studied are  $n = 4, 6$  and  $9$ , and these are universal since they occur for all alkali-halides and do not depend on the specific ground state geometry. Instead those numbers allow for the formation of compact clusters. Full geometrical relaxations are considered for  $(LiF)_n$  ( $n = 3 - 7$ ) and  $(AX)_3$  clusters, and the effect of Coulomb correlation is studied in a few selected cases. These two effects preserve the general conclusions achieved thus far.

## I. INTRODUCTION

Small clusters often present significant physical and chemical differences with respect to the bulk phase. While the structural possibilities are limited for the bulk material, the number of different isomers which may coexist for clusters is usually large, and the energy differences between isomers are often small. Here we are interested in neutral stoichiometric clusters of typical materials with ionic bonding, that is  $(AX)_n$  clusters, where  $A$  is an alkali and  $X$  a halide atom. As *ab initio* studies on these clusters are computationally expensive, the first theoretical calculations were based on pairwise interaction models<sup>1-3</sup>. Meanwhile, experimentalists moved forward using several techniques to produce and investigate these clusters: particle sputtering<sup>4,5</sup>, where rare-gas ions are used to bombard a crystal surface, vapor condensation in an inert-gas atmosphere<sup>6-8</sup>, and laser vaporization of a crystal surface<sup>9,10</sup>. In the expanding molecular jet conditions, clusters undergo a rapid and efficient evaporative cooling, and this leads to a cluster size distribution determined almost exclusively by the cluster stability. The evaporative cooling process leads to the so-called abundance magic numbers as a result of the longer time that the most stable clusters remain in the beam before decaying. Alkali halide magic numbers are often explained in terms of cuboid structures resembling fragments of the crystalline lattice, but other possibilities like ring stackings, or even mixed structures exist, which could be competitive. Nevertheless, only recently the possibility of detecting different isomers has emerged in drift tube experiments<sup>11,12</sup>. Those experiments have led to a renewed interest in isomerization studies. In order to disentangle these interesting problems, *ab initio* calculations<sup>13-16</sup> provide an ideal complement to the experimental studies, which are restricted to charged species. For instance, a study of  $(KCl)_n$  and  $(LiF)_n$  clusters up to sizes of  $n = 32$  has been carried out in ref. 16, using quantum-chemical methods including correlation effects at the MP2 level. We have performed calculations for  $(NaCl)_n$  and  $(NaI)_n$  using the *ab initio* Perturbed Ion (PI) model<sup>13,14</sup>.

The objective of the present paper is to give a global characterization of the structure and other related properties of small neutral alkali halide clusters. To this end we have carried out extensive PI calculations for the  $(AX)_n$  ( $n = 1 - 10$ ) clusters, identifying the most stable isomers, the binding energy differences between some isomers, and the evolution of several properties with the cluster size. Trends are highlighted and differences between different materials are discussed. To obtain a more profound insight on the physics behind the observed trends, the  $(AX)_6$  clusters are studied in more detail. Thus, conclusions can be drawn as to what energy components dictate the structure of the ground state isomer. Direct contact with the results of drift tube experiments is yet premature since those experiments involve nonstoichiometric singly-charged clusters.

This paper is structured as follows: Section II contains a brief account of the theoretical method and computational details. Section III contains the results for the structure and bonding properties. Section IV contains a detailed study of the  $(AX)_6$  clusters, which provides further insight on the results obtained in section III. Finally, section V contains our conclusions and summarizes the principal ideas of this study.

## II. METHOD

According to the Theory of Electronic Separability (TES)<sup>17,18</sup>, when a system is composed of weakly interacting groups, its wave function can be expressed as an antisymmetrized product of group wave functions. If these satisfy strong-orthogonality conditions<sup>19,20</sup>, the total energy can be written as a sum of intragroup energies and intergroup interaction energies. The Perturbed Ion (PI) model is a particular application of the TES in which each atom in a cluster with a fixed structure (or in a crystal) is considered as a different group<sup>21</sup>. The TES provides an efficient tool for dealing with ionic bonding<sup>22</sup>. Thus, alkali-halide clusters are ideal systems to be treated by the PI model. The ions (positive and negative) are the basic entities of the model. Their electronic structures are selfconsistently calculated, subject to the effect of the ion environment, by using an effective hamiltonian including intragroup terms and coulombic, exchange and projection ion-cluster interaction terms. The exchange interaction is accurately approximated by a nondiagonal spectral resolution, as given by Huzinaga *et al.*<sup>23</sup>. The projection energy term enforces strong orthogonality conditions between the ionic wave functions, increasing their kinetic energies and providing the short-range repulsive forces necessary for the stability of the cluster. All the two-center integrals involved in the calculation of these three interaction terms are analytically determined by using the algorithm of Silverstone and Moats for the expansion of a function around a displaced center<sup>24</sup>. The PI model is formulated at a Hartree-Fock (HF) level and has been described in full detail in other papers<sup>13,14,21</sup>. Correlation can also be included in an approximate way.

In the calculations we have used large multi-zeta Slater-Type Orbital (STO) basis sets, taken from Clementi and Roetti<sup>25</sup>. Basis sets optimized for the description of ions in vacuum are, in principle, an available choice to describe those ions in a cluster. However these are not necessarily the best basis sets, as shown in reference 13(c). The sensitivity of the PI model to the quality of the wave function tails is well documented<sup>21,22,26,27</sup>. Specifically, the effective potential for each ion depends, among other factors, on the overlaps with wave functions of neighbor ions. Thus, it is of paramount importance to choose the most appropriate basis set for the description of each material. We have performed exploratory studies for  $AX$  molecules and  $(AX)_6$  clusters. Specifically, we have used the basis sets of Clementi and Roetti with the exponents optimized for the description of ions in vacuum, and also with the exponents optimized for the neutral species. The main difference between these basis sets is indeed in the tail zone. This leads to four distinct possible basis sets for each alkali halide. The basis set leading to the largest binding energy for each individual alkali-halide material (the results for  $(AX)_6$  and  $AX$  lead to the same conclusions) has been adopted for all clusters of that material. We have also checked that inclusion of diffuse orbitals is not necessary.

## III. CLUSTER GEOMETRIES AND RELATIVE STABILITIES.

### A. Ground state structures and low-lying isomers

The problem of minimizing the total cluster energy with respect to the positions of all the ions is computationally very demanding. In our case we have performed a restricted search on the  $(3n-6)$ -dimensional potential energy-surface. The starting geometries have been investigated by other authors<sup>1-3</sup> within the context of pair potential models. Specifically, we have considered cuboid structures (rock-salt fragments), ring-like configurations (mainly hexagonal) together with prismatic structures obtained by stacking those rings, and some mixed configurations. For the cuboid-like structures, the energy has been minimized with respect to a single parameter, the nearest neighbor distance. For ring-like structures, we have relaxed two or three parameters, one accounting for the stacking distance between parallel rings and the two others for the different distances of cations and anions to the center of the ring.

Figure 1 shows the results for  $(LiF)_n$  and  $(KCl)_n$  clusters. The ground state and one or more low-lying isomers are given for each  $n$ . The energy difference with respect to the most stable isomer is given (in eV) below each isomer. The first number corresponds to  $(KCl)_n$  and the number below to  $(LiF)_n$ . Although we have performed calculations for many alkali-halides, we only represent in Fig. 1 the results for  $(KCl)_n$  and  $(LiF)_n$  because those two systems show well the main trend in structural stability, namely the competition between rings and stacks of rings (mainly hexagonal) on one hand, and structures that are fragments of a rock-salt crystal lattice on the other. The tendency to form rings is stronger in  $(LiF)_n$ , and most  $(KCl)_n$  clusters form instead rock-salt fragments. These structural trends

support the conclusion of Ochsenfeld and Ahlrichs<sup>16</sup> of a slower convergence of  $(LiF)_n$  towards bulk properties. More generally, all alkali-halide clusters containing  $Li$  have a tendency to form rings, clusters containing  $K$  and  $Rb$  form rock-salt pieces, and  $Na$ -halides represent an intermediate case. Of course there are exceptions to this simple rule: for instance, we observe in fig. 1 that the lowest energy structure of  $(LiF)_7$  and  $(KCl)_7$  is in both cases a fragment of the wurtzite crystal. Also, the ground state structure for  $n = 3$  is the hexagonal ring in both systems.

To give a more precise description of the competition between ring-like and cuboid isomers we present in fig. 2 an structural stability map in which the two coordinates are the empirical anion ( $r_A$ ) and cation ( $r_C$ ) radii<sup>28</sup>. The map corresponds to  $(AX)_6$ , and the straight line drawn in the map achieves a perfect separation between the systems in which the lowest structure is the cuboid and those that prefer the hexagonal prism. The same line separates the hexagonal prism and the rock-salt fragment in  $(AX)_9$ , but the line may depend a little on  $n$ : a vertical line neatly separating  $Li$  clusters from the rest serves to distinguish between the octagonal ring and the cube in  $(AX)_4$ . The conclusion from the structural maps is that two parameters,  $r_A$  and  $r_C$ , are enough to parametrize the competition between ring-like and rock-salt isomers: alkali-halide clusters with a small  $r_C$  and a large  $r_A$  have a tendency to form rings, although the first requirement (small  $r_C$ ) is almost sufficient.

The ring versus rock-salt competition can be further simplified to a one-parameter plot. In fig. 3 the energy difference between the two isomers has been plotted versus the ratio  $r_C/r_A$ , again for  $n = 6$ . A visible correlation exists between the two magnitudes. A critical ratio  $r_C/r_A = 0.5$  separates the hexagonal from the rock-salt structures.

### B. Evolution of the interionic distances with cluster size

In figure 4 we present the evolution of the averaged interionic distances of  $(LiF)_n$  and  $(KCl)_n$  with the cluster size for two isomeric families (rock-salt and hexagonal prism). The tendency is a slight increase of the cation-anion distance  $d$  with cluster size, but each isomeric family follows a different growth curve and cation-anion distances are smaller in the hexagonal-ring pieces. Although not plotted in the figure we have found that interionic distances in higher order rings (octagonal, ...) are even smaller, so we conclude that the higher the order of the rings forming the structure, the smaller the interionic distances.  $d$  tends to a saturation value in cubic  $(KCl)_n$  clusters which is about  $0.1 \text{ \AA}$  larger than the corresponding interionic bulk distance  $d(KCl) = 3.33 \text{ \AA}$ <sup>28</sup>. In cubic  $(LiF)_n$  clusters, on the other hand,  $d$  tends from below to a value very close to the corresponding bulk limit  $d(LiF) = 2.02 \text{ \AA}$ .

### C. Cluster Stabilities

Now we examine the relative stability as a function of the cluster size. The binding energy per molecule of a given cluster  $(AX)_n$  with respect to the separate free ions is given by:

$$E_{bind} = \frac{1}{n} [nE_0(X^-) + nE_0(A^+) - E(cluster)], \quad (1)$$

where  $E_0$  refers to the energies of the free ions. In figure 5 we show  $E_{bind}$  as a function of  $n$ , for a number of alkali-halides. The general trend is an increase of  $E_{bind}$  with  $n$ . However, some values of  $n$  for which the cluster is specially stable can be observed. These are  $n = (4), 6$  and  $9$ . Local maxima can be seen for  $n = 6, 9$  in all cases, and a maximum or a change of the slope of the curve for  $n = 4$ . The most important feature is that these magic numbers are “universal” within the alkali-halide family, that is, they occur both in ring-forming systems and in rock-salt forming systems and this occurs because the difference in energy between ring-like and rock-salt isomers is small compared to the change in binding energy when the cluster size  $2n$  changes. In summary, it is the especial value of  $n$  that makes some clusters special and not their particular ground state geometries. The stability occurs because those special sizes permit the formation of “compact” clusters. Let us illustrate this with specific examples. The two isomers of  $(AX)_5$  (a decagonal ring and a cube with an  $AX$  molecule attached to it) and the hexagonal isomers of  $(AX)_7$  contain some low coordinated ions, in contrast to  $(AX)_6$ .  $(AX)_9$  is also more compact than the elongated forms of  $(AX)_{10}$  and  $(AX)_8$ . The octagonal prism in  $(AX)_8$  contains also less coordinated ions than  $(AX)_9$ . This idea of stability of compact clusters is evidently associated to the optimization of the attractive part of the electrostatic energy. Excluding the lithium clusters, our results are in accordance with a geometrical model<sup>1,2</sup> proposed to explain the magic numbers of large clusters with ionic bonding. This model assumes that the most stable configurations correspond to those values of  $n$  for which it is possible to form compact cuboid structures of type  $(a \times b \times c)$ , where  $a$ ,  $b$  and  $c$  are the number of atoms along three perpendicular edges.

## D. Inclusion of general geometrical distortions

In addition to the restricted search of energy minima described in Section III-A above, we have performed “full geometrical relaxations” for  $(LiF)_n$  ( $n \leq 7$ ) and for all the  $(AX)_3$  clusters. To this end, we have used a simplex downhill algorithm<sup>29,30</sup>. The input geometries for these additional calculations are those obtained from the previous restricted calculations. Results for  $(LiF)_n$  ( $n = 3 - 7$ ) are presented in figure 6. Appreciable distortions are observed in some low-lying isomers but not on the ground state. The effect of the distortions is to reduce the energy difference between the first isomer and the ground state, although the relative ordering of these two is not changed. The effect is largest for  $n = 5$ , where the energy difference between isomers is lowered by 3.39 eV. For  $n = 4$ , the ring remains as the lowest energy structure, but the isomers are now nearly degenerate. For other materials we have performed such calculations only for  $n = 3$ , and the distortions are very small. The general conclusion of this section is the same as in Section III-A, namely, that only  $(LiX)_n$  and some  $(NaX)_n$  clusters have a marked tendency to adopt ringlike structures.

## E. Inclusion of correlation effects

Coulomb correlation can play a significant role when the HF energy differences between isomers are small. We have studied the influence of correlation in some selected cases by using the unrelaxed Coulomb-Hartree-Fock (uCHF) model proposed by Clementi<sup>31,32</sup>. Within this model, the PI wave functions calculated at the HF level are kept fixed and the correlation energy is added as a (perturbative-like) correction. The calculations have been carried out using the restricted search described in section III A. As the electron-electron repulsion is lowered upon inclusion of correlation, a contraction of the interionic distances is obtained in all cases. This contraction is always larger in the more compact (rock-salt) isomer compared to the ring-like isomers. Results for the effect on the binding energies of  $(LiX)_4$  clusters are presented in Table I. The inclusion of correlation leads to higher binding energies and results in a larger stabilization of the cube isomer. This reduces the energy difference between the two isomers in  $(LiCl)_4$ ,  $(LiBr)_4$ ,  $(LiI)_4$ , and it changes the order of the two isomers in  $(LiF)_4$ , giving a result in accordance with those of references 16,33, where a cube was obtained as the most stable  $(LiF)_4$  isomer. However,  $(LiCl)_4$ ,  $(LiBr)_4$  and  $(LiI)_4$  remain as octagonal rings. Thus, the stability map for  $n = 4$  only changes gently and its main characteristics remain valid upon inclusion of correlation.

We have also performed uCHF calculations for the planar  $(KX)_3$  isomers, and the results are given in Table II. The most stable structure for  $(KX)_3$  at the HF level is the hexagonal ring, the same obtained for  $(NaCl)_3$  in references 13,15 and for  $(NaI)_3$  in reference 14. The calculations of Ochsenfeld *et al.*<sup>16</sup> predict that the rectangular (or double chain) structure becomes the most stable  $(KCl)_3$  isomer upon inclusion of correlation at the MP2 level. We do not obtain the double chain as the minimum energy isomer of the  $(KX)_3$  clusters upon including correlation, but the energy differences between the two isomers decrease a little. For instance, the energy difference for  $(KCl)_3$  changes from 0.05 eV at the HF level to 0.04 eV at the uCHF level. On the other hand, if we perform a uCHF calculation for the fixed geometries of  $(KX)_3$  isomers fully relaxed at the HF level, the above energy differences are 0.14 (HF) and 0.11 eV (uCHF), respectively. Thus, inclusion of correlation and a full geometrical relaxation have opposite effects on the relative stability of the two isomers. The main conclusion is that both isomers could coexist in the experiments, since their energies are close.

From figure 3 it can be appreciated that the two  $(NaBr)_6$  isomers have nearly the same energy. Inclusion of Coulomb correlation inverts the order of the isomers only in this case. Thus, the general features of the stability map remain valid after including correlation. In summary, inclusion of Coulomb correlation results in a gain in binding energy which is larger for the rock-salt isomers, but this effect becomes significant only for those cases showing near degenerate isomers.

## IV. DETAILED STUDY OF THE $(AX)_6$ ISOMERS.

### A. Hexagonal versus rock-salt isomer

In this section we deal with the specific case of  $n = 6$  and work at the level of restricted relaxation explained in section III A. Our goal is to achieve a deeper understanding of the stability map presented in fig. 2. To this end we have analysed the factors giving rise to the cluster binding energy. In order to study the deformations on the electron density of the ions induced by the cluster environment we have calculated the expectation value  $\langle r^2 \rangle_{nl}$  for all the geometrically-inequivalent ions in the cluster. That expectation value is taken over the outermost occupied

ionic orbital  $\psi_{nl}$ . In Table III, the values of  $\langle r^2 \rangle_{nl}$  for  $F^-$  and  $I^-$  anions in vacuum and in some  $(AX)_6$  clusters are compared. Ions in the hexagonal prism are labelled with the letter  $r$  (ring). In the rock-salt cluster there are two nonequivalent sites, labelled  $c$  (corner) and  $e$  (edge). The orbital contraction is important. For a fixed anion, the contraction is the largest for the  $Li$  halide. In contrast, the contraction of the cationic orbitals is negligible.

It can be shown<sup>13,14,21</sup> that the binding energy of equation (1) can be written as:

$$nE_{bind} = \sum_R E_{bind}^R = - \sum_R (E_{def}^R + \frac{1}{2} E_{int}^R), \quad (2)$$

where the sum runs over all the ions in the cluster. According to this equation we can separate the binding energy into a sum of site contributions, each one composed in turn of two terms.  $E_{def}^R$  accounts for the self-energy associated to the deformation of the wave functions of the free ions by the cluster environment, so it is related to the change of  $\langle r^2 \rangle_{nl}$  and depends on the specific site in the cluster.  $E_{int}^R$  is the interaction energy of the ion  $R$  with the rest of the cluster, namely  $E_{int}^R = E_{class}^R + E_{nc}^R + E_X^R + E_{overlap}^R$ , where the different terms are respectively: the electrostatic interaction between the ion  $R$  and the other ions of the cluster, considered as point charges, the correction to this classical energy due to the finite extension of the wave functions, the exchange part of the interaction energy, and the overlap energy<sup>34</sup>. Thus, after performing the  $R$ -sum, the binding energy can accordingly be partitioned as:

$$nE_{bind} = E_{def} + \frac{1}{2} E_{class} + \frac{1}{2} (E_{nc} + E_X + E_{overlap}) = E_{def} + \frac{1}{2} E_{int}^{classical} + \frac{1}{2} E_{int}^{quantum}. \quad (3)$$

The deformation term is always positive<sup>13,14</sup>, so it opposes binding. The overlap contribution dominates  $E_{int}^{quantum}$ , so this term is also positive in all cases. Finally  $E_{int}^{classical}$ , which is the Madelung interaction energy between point-like charges, is negative and stabilises the cluster. It is worth to remark that all these energy components are obtained in a global selfconsistent process and that this partition of the binding energy is not strictly necessary; nevertheless, it proves conceptually quite useful.

Now, the difference in binding energy per molecule between the hexagonal and rock-salt  $(AX)_6$  isomers can be analysed in those three components. That is made in Table IV. The following trends can be appreciated: (a) The deformation part always favors the hexagonal isomer. (b) The interionic distances are smaller in the hexagonal isomer and therefore the overlap is larger. Consequently the term involving overlap favors the rock-salt isomer. (c)  $E_{int}^{classical}$  already displays the main feature of figure 3, that is, the distinction between the hexagonal and the rock-salt fragment. This is very interesting because a classical Madelung interaction would favor the cuboid isomer if the interionic distances were the same in both isomers. The Madelung energy becomes more negative for the hexagonal prism only if the interionic distance  $d(hex)$  is smaller than a critical fraction  $\alpha d(cube)$  of the interionic distance in the cube isomer, with  $\alpha$  a number slightly smaller than 1. This occurs for those materials with  $r_C/r_A \leq 0.5$ . Although the stability map can then be justified in terms of classical energy components, the equilibrium interionic distance, which is a key factor in this discussion, results from a delicate balance between all the energy components, classical and nonclassical. Returning to the borderline case  $(NaBr)_6$ , the inclusion of Coulomb correlation induces a contraction of the interionic distances in both isomers, but this contraction is larger for the rock-salt isomer, and the Madelung energy produces an inversion in the order of the two isomers.

## B. Additional geometrical relaxation of the cuboid isomer

A better description of the structure of the rock-salt isomer is obtained by allowing inequivalent ions to relax independently. We have then relaxed the geometry with respect to four parameters, the distances from the cluster center to the four inequivalent ion types (corner and edge cations and corner and edge anions). In all the  $Li$  compounds and in  $(NaI)_6$ , cations tend to move inwards, while anions move outwards, producing slight deformations. This situation is reversed for the rest of clusters, in which cations move outwards and anions move inwards. The deformations have an interesting effect on the effective ion size. To see this effect we have calculated again  $\langle r^2 \rangle_{nl}$  for the outermost orbital of each ion. Compared to the results for rock-salt isomers of Table III we have now obtained almost identical contractions for the electronic clouds of anions at inequivalent (corner, edge) sites, with the conclusion that anions at inequivalent positions have, nevertheless, an identical size. The size changes, however, with the nature of the alkali partner.

## V. CONCLUSIONS

Using the perturbed ion (PI) model, we have calculated the most stable structures of neutral alkali-halide clusters  $(AX)_n$ , with  $n \leq 10$ ,  $A = Li^+, Na^+, K^+, Rb^+$  and  $X = F^-, Cl^-, Br^-, I^-$ . With few exceptions, the equilibrium geometries obtained are ringlike structures for  $(LiX)_n$  and  $(NaI)_n$  clusters, and rock-salt fragments for the rest of materials;  $(NaBr)_6$  is a borderline case. The competition between rock-salt and ring-like isomers has been studied in detail and we have found that a stability map with two parameters (the cationic and anionic ionic radii) is able to separate the alkali-halides in two well-defined structural families. A further simplification to a one-parameter ( $r_C/r_A$ ) plot has been possible, from which an approximate value of 0.5 has been extracted that separates the two families. The interionic distances show a smooth variation with the number of molecules in the cluster when different structural families are considered separately. The alkali-halide magic numbers have an universal character, based on the fact that highly compact isomers can be built with a number of molecules equal to 4, 6 and 9. Additional calculations allowing for full geometrical relaxations have been performed in the case of  $(LiF)_n$  ( $n = 3 - 7$ ) and  $(AX)_3$  clusters. *Li*-based clusters show larger geometrical distortions than clusters non-containing lithium. The structures have been compared with those obtained from other theoretical calculations, and the overall agreement is good. Inclusion of correlation corrections has been considered only in those cases with near-degenerate isomers.

The partition of the binding energy for the  $(AX)_6$  clusters has shown that the key ingredients to understand the structural differences of figures 2 and 3 are the cation-anion distances and the classical electrostatic Madelung contribution.

To sum up, a simple picture emerges to explain the observed structural trends: when the ratio  $r_C/r_A \leq 0.5$ , the interionic distances at equilibrium, determined by minimization of the *total* energy, are such that the classical Madelung interaction between point-like ions favors the hexagonal isomer. On the other hand, when  $r_C/r_A > 0.5$ , the interionic distances produce Madelung energies favoring rock-salt structures.

**ACKNOWLEDGMENTS:** Work supported by DGES (PB95-0720-C02-01) and Junta de Castilla y León (VA25/95). A. Aguado is supported by a predoctoral fellowship from DGES.

## Captions of tables

**Table I.** Effect of correlation on the binding energies of  $(LiX)_4$  clusters. HF and uCHF binding energies per molecule are given (in eV) for the cube and the octogonal ring.

**Table II.** Effect of correlation on the binding energies of planar  $(KX)_3$  clusters. HF and uCHF binding energies per molecule are given (in eV) for the double chain and the hexagonal ring.

**Table III.** Values of  $\langle r^2 \rangle_{nl}$  in a.u. for the outermost occupied orbitals of  $F^-$  and  $I^-$  anions in vacuum and in four representative  $(AX)_6$  clusters. r: ring site; c: corner site; e: edge site (as defined in the text).

**Table IV.** Difference in binding energy per molecule between rock-salt and hexagonal  $(AX)_6$  isomers, together with their partition in deformation, quantum and classical interaction terms, as defined in the text. A minus sign indicates that the corresponding quantity favors the hexagonal isomer. All quantities in eV.

Material	$(LiF)_4$		$(LiCl)_4$		$(LiBr)_4$		$(LiI)_4$	
	HF	uCHF	HF	uCHF	HF	uCHF	HF	uCHF
Cube	8.99	9.67	6.88	7.49	6.47	7.30	5.74	6.53
Ring	9.00	9.59	7.00	7.52	6.56	7.32	5.91	6.57

TABLE I.

Material	$(KF)_3$		$(KCl)_3$		$(KBr)_3$		$(KI)_3$	
	HF	uCHF	HF	uCHF	HF	uCHF	HF	uCHF
Double-chain	6.41	6.88	5.25	5.75	5.06	5.70	4.63	5.33
Ring	6.47	6.92	5.30	5.79	5.10	5.72	4.67	5.35

TABLE II.

	Site	$\langle r^2 \rangle_{nl}$		Site	$\langle r^2 \rangle_{nl}$
$F^-$ : gas phase		2.207	$I^-$ : gas phase		8.621
$F^-$ : $(LiF)_6$	<i>r</i>	1.794	$I^-$ : $(LiI)_6$	<i>r</i>	7.575
	<i>c</i>	1.806		<i>c</i>	7.604
	<i>e</i>	1.763		<i>e</i>	7.398
$F^-$ : $(RbF)_6$	<i>r</i>	1.899	$I^-$ : $(RbI)_6$	<i>r</i>	7.779
	<i>c</i>	1.907		<i>c</i>	7.789
	<i>e</i>	1.867		<i>e</i>	7.645

TABLE III.

Material	$\Delta E_{def}$	$\frac{1}{2}\Delta E_{int}^{quantum}$	$\frac{1}{2}\Delta E_{int}^{classical}$	$\Delta E_{bind}$
<i>LiI</i>	-0.069	0.048	-0.089	-0.110
<i>LiBr</i>	-0.058	0.048	-0.081	-0.091
<i>LiCl</i>	-0.061	0.059	-0.088	-0.090
<i>LiF</i>	-0.067	0.098	-0.103	-0.072
<i>NaI</i>	-0.034	0.055	-0.041	-0.020
<i>NaBr</i>	-0.023	0.045	-0.023	-0.001
<i>NaCl</i>	-0.031	0.033	0.003	0.005
<i>NaF</i>	-0.046	0.064	0.006	0.024
<i>KI</i>	-0.034	0.022	0.028	0.016
<i>KBr</i>	-0.022	0.013	0.029	0.020
<i>KCl</i>	-0.008	0.017	0.013	0.022
<i>KF</i>	-0.039	0.055	0.015	0.031
<i>RbI</i>	-0.034	0.014	0.044	0.024
<i>RbBr</i>	-0.009	0.021	0.014	0.026
<i>RbCl</i>	-0.001	0.020	0.008	0.027
<i>RbF</i>	-0.025	0.033	0.027	0.035

TABLE IV.



## Captions of figures

**Figure 1.** Lowest-energy structures and low-lying isomers of  $(LiF)_n$  and  $(KCl)_n$  clusters, relaxed as indicated in the text. The energy difference (in eV) with respect to the most stable structure is given below the corresponding isomers. First row:  $KCl$ ; second row:  $LiF$ . Stability decreases from left to right for  $(KCl)_n$  clusters.

**Figure 2.** Structural stability map for  $(AX)_6$ . A plot in terms of the cation and anion radii,  $r_C$  and  $r_A$  respectively, separates the hexagonal (squares) from the cubic (circles) isomers. The same map is also valid for  $(AX)_9$ .

**Figure 3.** Energy difference between hexagonal and rock-salt isomers in  $(AX)_6$  versus the ratio of ionic radii.

**Figure 4.** Interionic distances in  $(LiF)_n$  (open circles) and  $(KCl)_n$  (full circles) clusters. Lines join isomers pertaining to the same structural family: rock-salt (full line), hexagonal rings (dashed line). Left scale is for  $(LiF)_n$  and right scale for  $(KCl)_n$ .

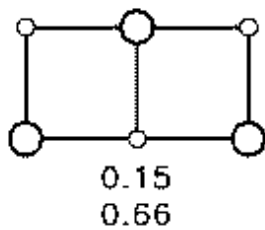
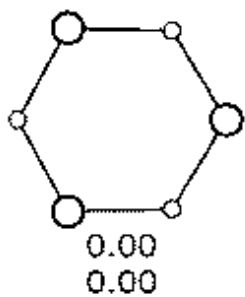
**Figure 5.** Binding energy per molecule as a function of the cluster size for some alkali-halide clusters. From the top to the bottom, these are:  $LiCl$ ,  $LiBr$ ,  $RbF$ ,  $NaBr$ ,  $LiI$ ,  $KCl$ ,  $KBr$ ,  $RbCl$ ,  $RbBr$ ,  $KI$ , and  $RbI$ .

**Figure 6.** Lowest-energy structures and low-lying isomers of  $(LiF)_n$  ( $n = 3 - 7$ ) calculated allowing for a full geometrical relaxation. Differences in total energy are given in eV.

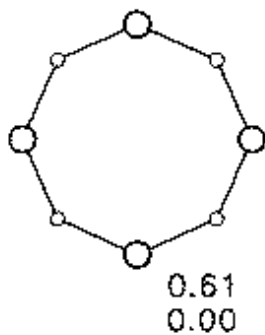
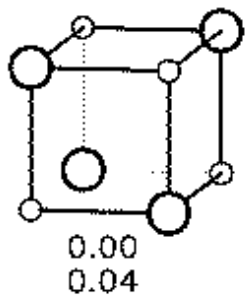
- 
- <sup>1</sup> T. P. Martin, Phys. Rep. **95**, 167 (1983).
- <sup>2</sup> J. Diefenbach and T. P. Martin, J. Chem. Phys. **83**, 4585 (1985).
- <sup>3</sup> N. G. Phillips, C. W. S. Conover and L. A. Bloomfield, J. Chem. Phys. **83**, 4585 (1991).
- <sup>4</sup> J. E. Campana, T. M. Barlak, R. J. Colton, J. J. De Corpo, J. J. Wyatt and B. I. Dunlap, Phys. Rev. Lett. **47**, 1046 (1981).
- <sup>5</sup> T. M. Barlak, J. J. Wyatt, R. J. Colton, J. J. De Corpo, and J. E. Campana, J. Am. Chem. Soc. **104**, 1212 (1982).
- <sup>6</sup> O. Echt, K. Sattler and E. Recknagel, Phys. Rev. Lett. **47**, 1121 (1981).
- <sup>7</sup> R. Pflaum, P. Pfau, K. Sattler and E. Recknagel, Surf. Sci. **156**, 165 (1985).
- <sup>8</sup> R. Pflaum, K. Sattler and E. Recknagel, Phys. Rev. B **33**, 1522 (1986).
- <sup>9</sup> C. W. S. Conover, Y. A. Yang and L. A. Bloomfield, Phys. Rev. B **38**, 3517 (1988).
- <sup>10</sup> Y. T. Twu, C. W. S. Conover, Y. A. Yang and L. A. Bloomfield, Phys. Rev. B **42**, 5306 (1990).
- <sup>11</sup> M. F. Jarrold, J. Phys. Chem. **99**, 11 (1995).
- <sup>12</sup> M. Maier-Borst, P. Löffler, J. Petry and D. Kreisler, Z. Phys. D **40**, 476 (1997).
- <sup>13</sup> A. Ayuela, J.M. López, J.A. Alonso and V. Luaña, [a] Z. Phys. D **26**, S213 (1993); [b] An. Fis. (Spain) **90**, 190 (1994); [c] Physica B **212**, 329 (1995).
- <sup>14</sup> A. Aguado, A. Ayuela, J.M. López and J.A. Alonso, J. Phys. Chem. **101B**, 5944 (1997).
- <sup>15</sup> P. Weiss, C. Ochsenfeld, R. Ahlrichs, and M. M. Kappes, J. Chem. Phys. **97**, 2533 (1992); C. Ochsenfeld and R. Ahlrichs, *ibid.* **97**, 3487 (1992).
- <sup>16</sup> C. Ochsenfeld and R. Ahlrichs, Ber. Bunsenges Phys. Chem. **98**, 34 (1994).
- <sup>17</sup> S. Huzinaga and A. P. Cantu, J. Chem. Phys. **55**, 5543 (1971).
- <sup>18</sup> V. Luaña. *Thesis Dissertation*, Universidad de Oviedo (1987).
- <sup>19</sup> P. G. Lykos and R. G. Parr, J. Chem. Phys. **24**, 1166 (1956).
- <sup>20</sup> R. G. Parr, R. O. Ellison and P. G. Lykos, J. Chem. Phys. **24**, 1106 (1956).
- <sup>21</sup> V. Luaña and L. Pueyo, Phys. Rev. B **41**, 3800 (1990).
- <sup>22</sup> R. McWeeny, *Methods of molecular quantum mechanics*, Academic Press, London (1994).
- <sup>23</sup> S. Huzinaga, L. Seijo, Z. Barandiaran and M. Klobukowski, J. Chem. Phys. **86**, 2132 (1987).
- <sup>24</sup> A. Martín Pendás and E. Francisco, Phys. Rev. A **43**, 3384 (1991).
- <sup>25</sup> E. Clementi and C. Roetti, At. Data and Nuc. Data Tables **14**, 3 (1974); **14**, 177 (1974).
- <sup>26</sup> G. Höjler and J. Chung, Int. J. Quantum Chem. **14**, 623 (1978).
- <sup>27</sup> A. Martín Pendás, E. Francisco and J. M. Recio, J. Chem. Phys. **97**, 452 (1992).
- <sup>28</sup> N. M. Ashcroft and N. D. Mermin, *Solid State Physics*, Holt, Rinehart and Winston, New York (1976).
- <sup>29</sup> J. A. Nelder and R. Mead, Comput. J. **7**, 308 (1965).
- <sup>30</sup> W. H. Press and S. A. Teukolsky, Computers in Physics, **5**, 426 (1991).
- <sup>31</sup> E. Clementi, IBM J. Res. Develop. **9**, 2 (1965).
- <sup>32</sup> S. J. Chakravorty and E. Clementi, Phys. Rev. A **39**, 2290 (1989).
- <sup>33</sup> A. Heidenreich and J. Sauer, Z. Phys. D **35**, 279 (1995).
- <sup>34</sup> E. Francisco, A. Martín Pendás and W. H. Adams, J. Chem. Phys. **97**, 6504 (1992).

n

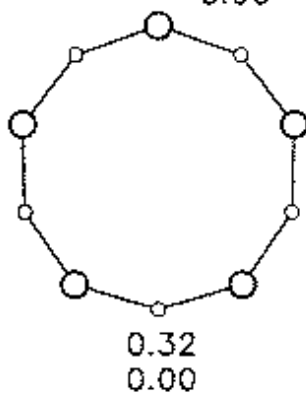
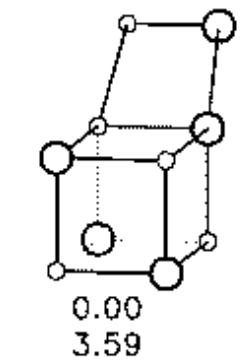
3



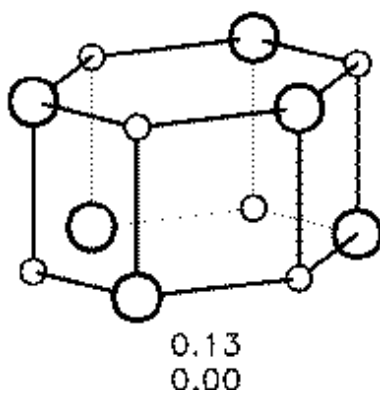
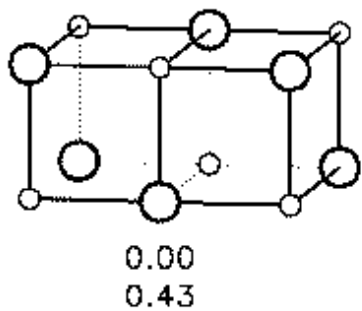
4



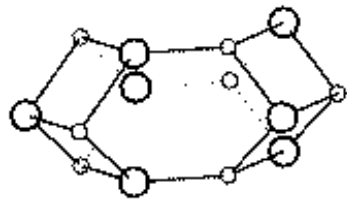
5



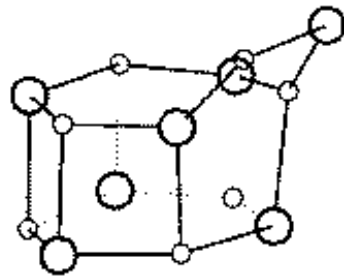
6



n

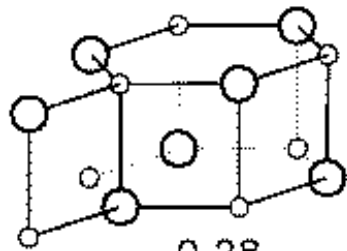


0.00  
0.00

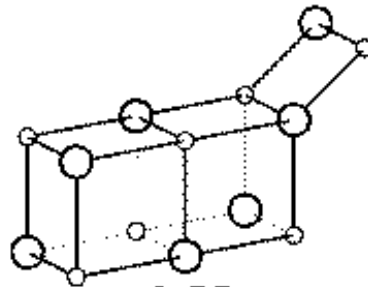


0.22  
0.17

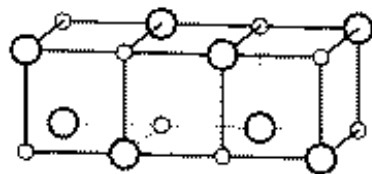
7



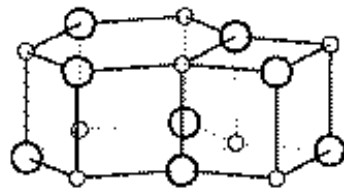
0.28  
0.30



0.53  
0.21

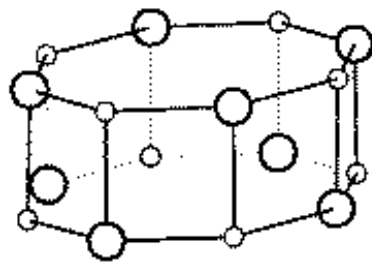


0.00  
0.15

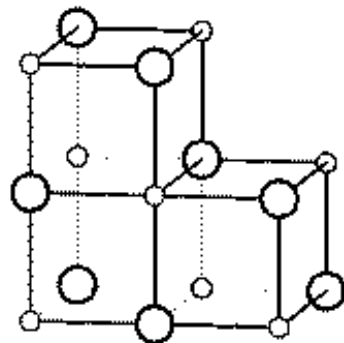


0.20  
0.13

8



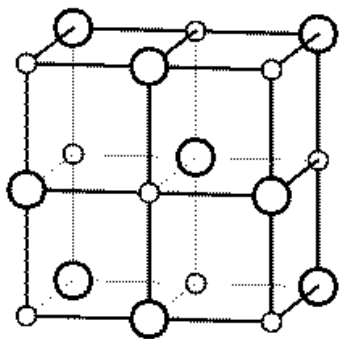
0.30  
0.00



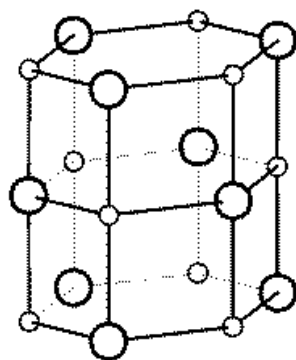
0.63  
1.24

n

9

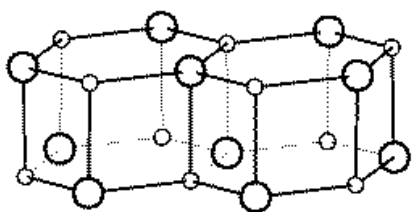


0.00  
0.47

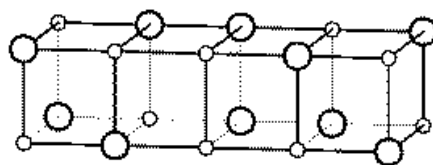


0.04  
0.00

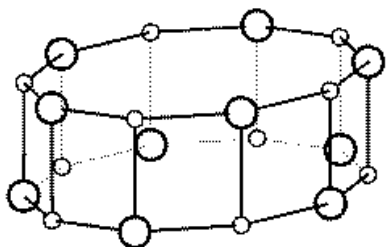
10



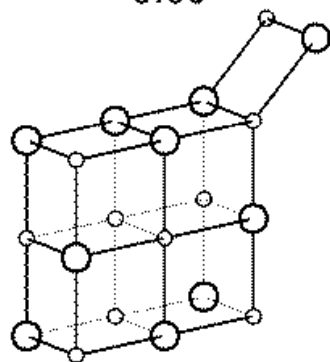
0.00  
0.00



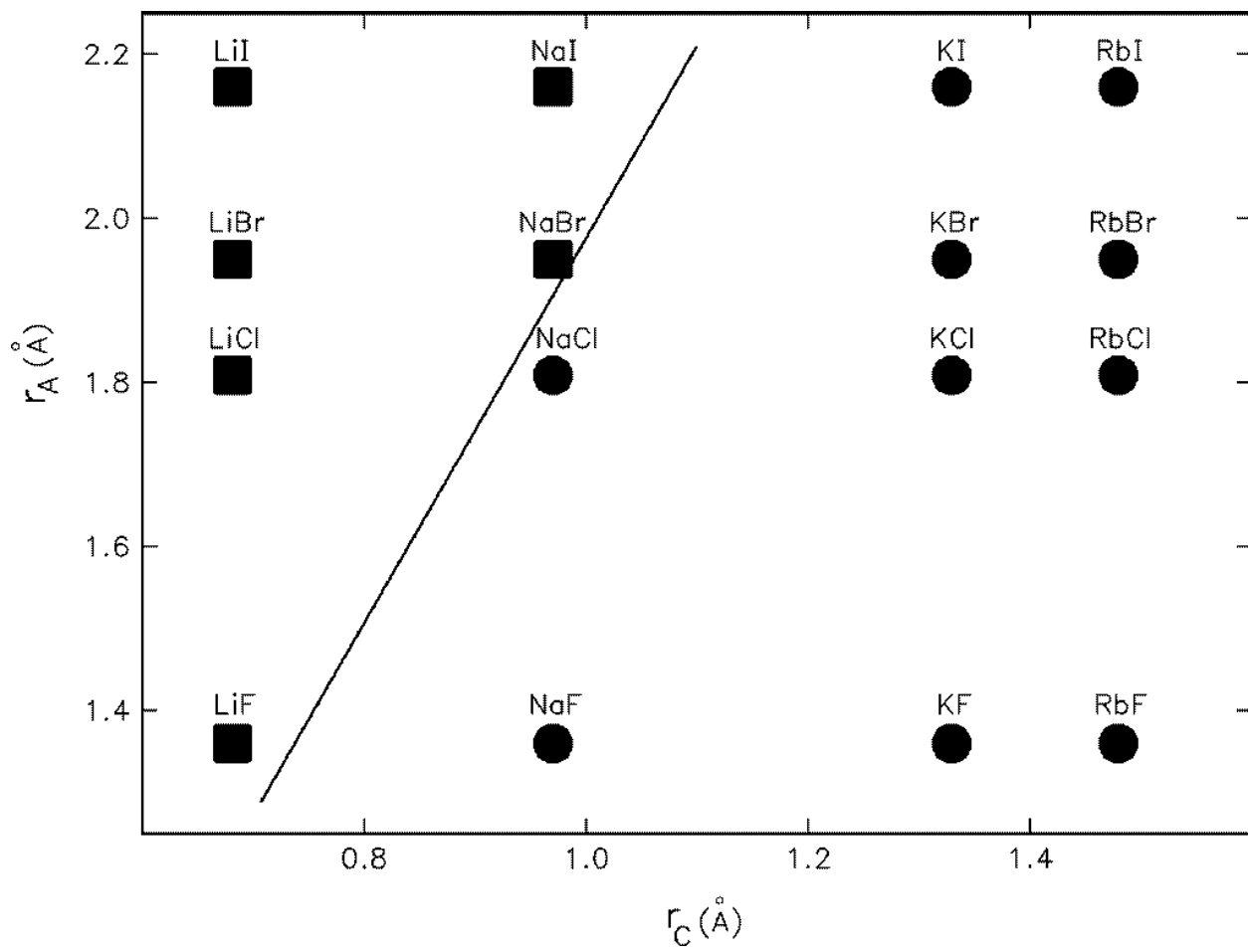
0.37  
0.09

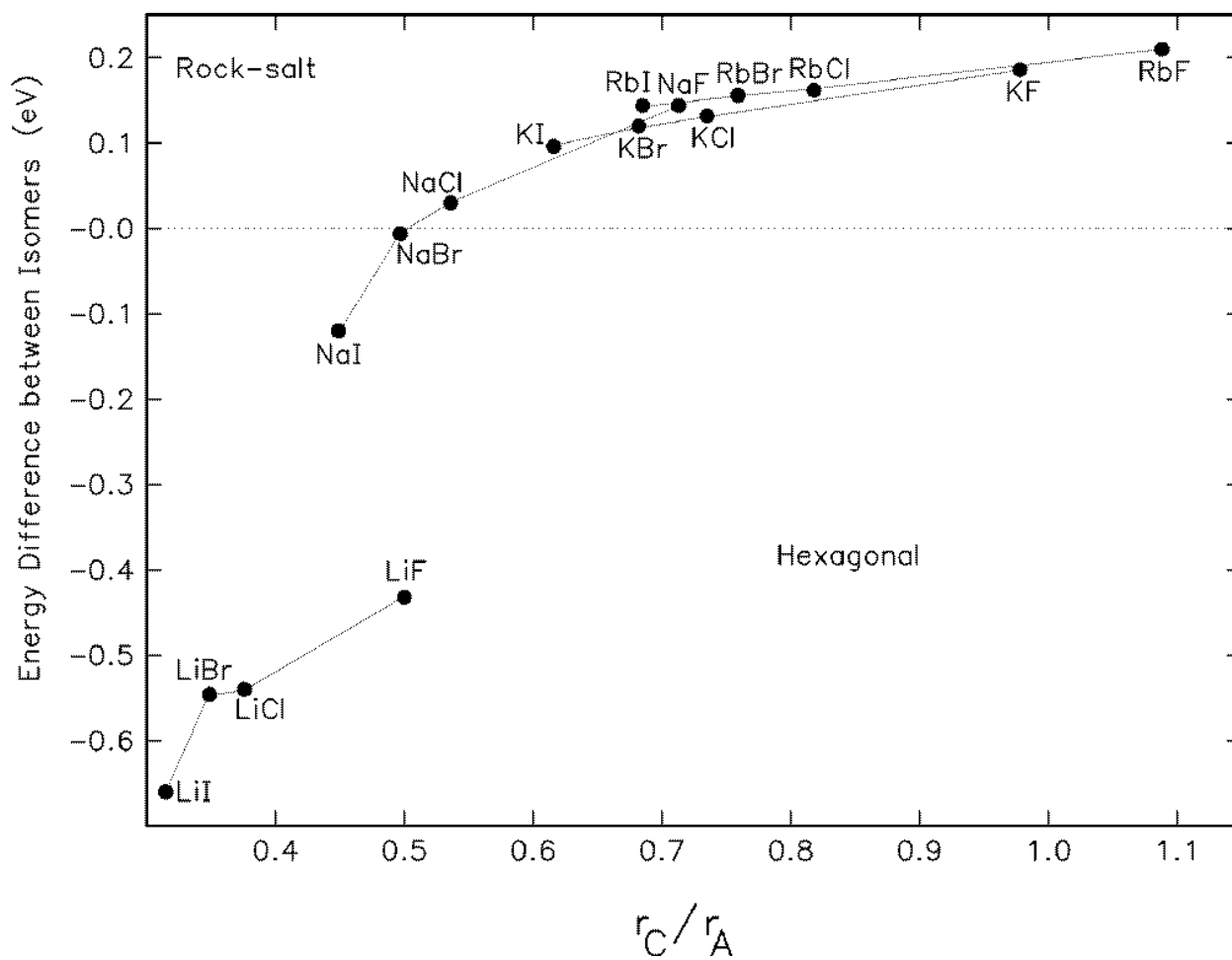


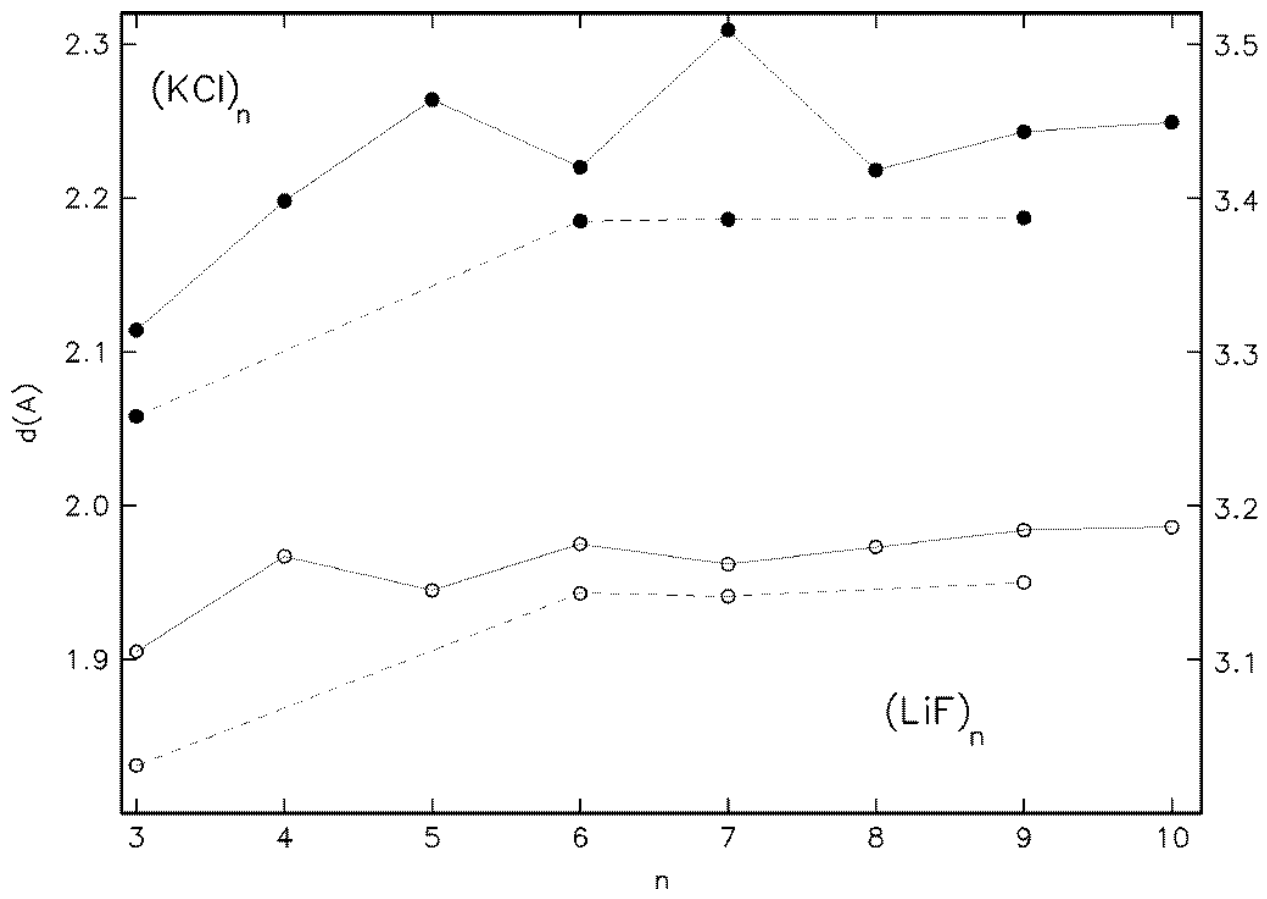
0.49  
0.26



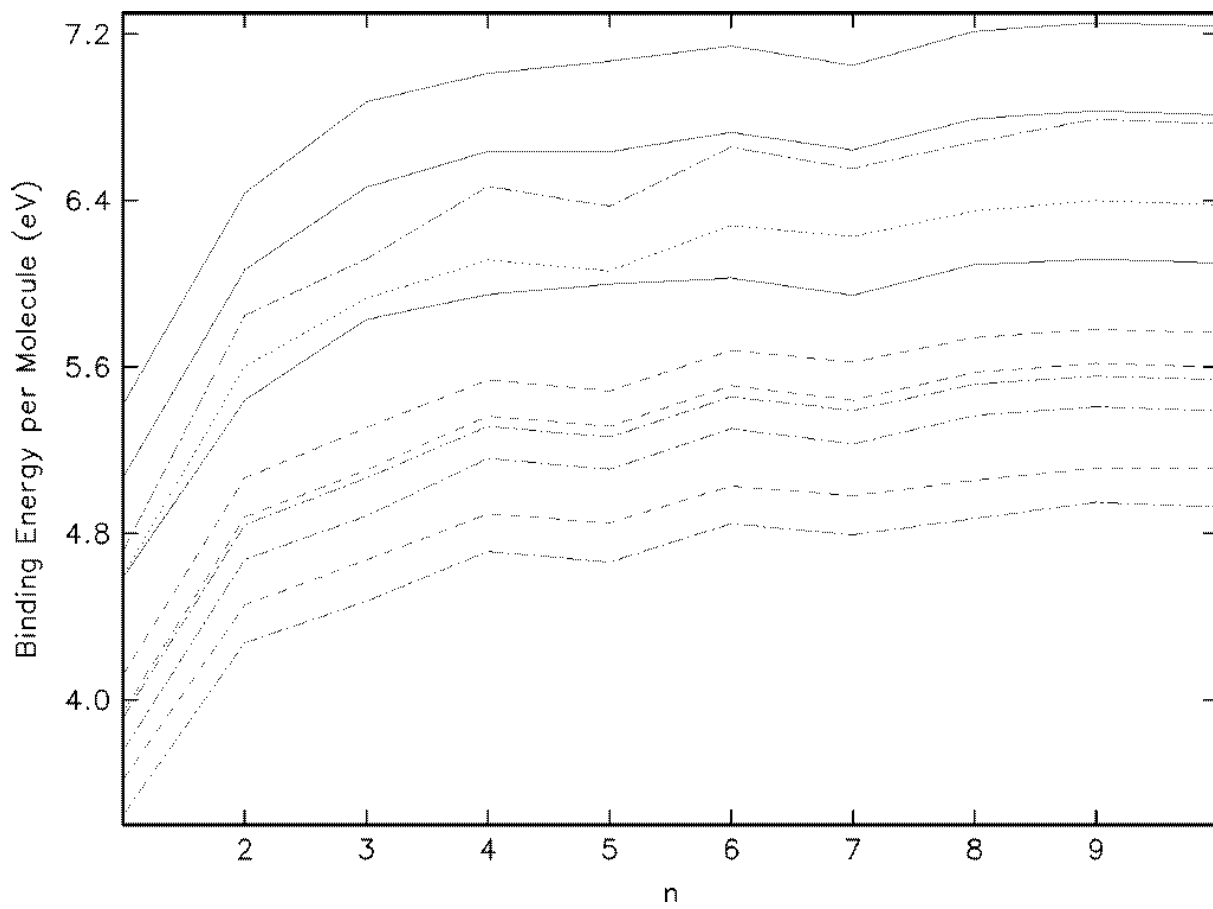
0.64  
0.45





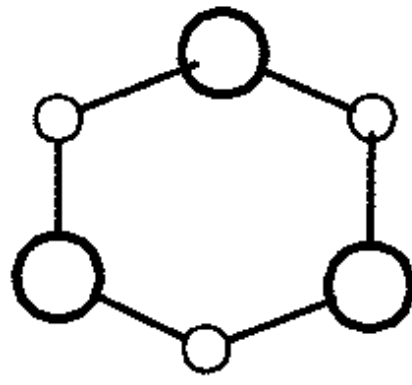
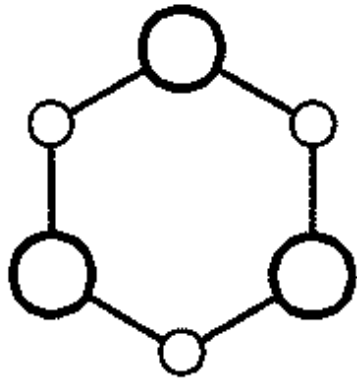






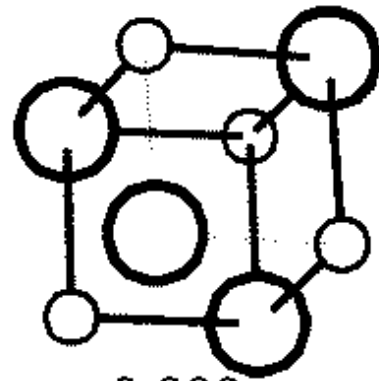
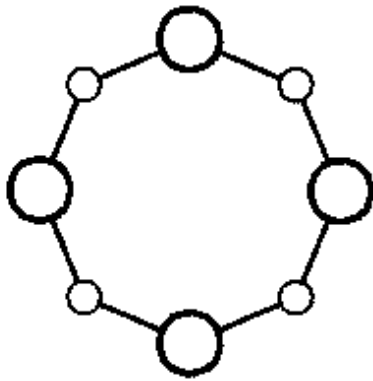
n

3



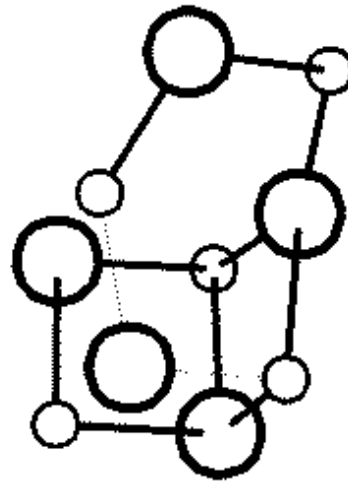
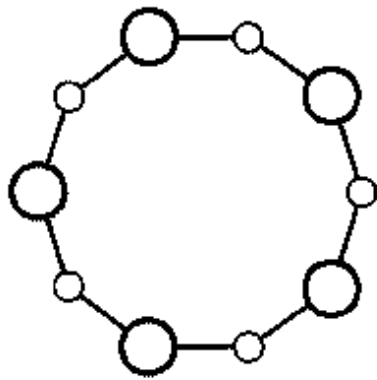
0.20

4



0.009

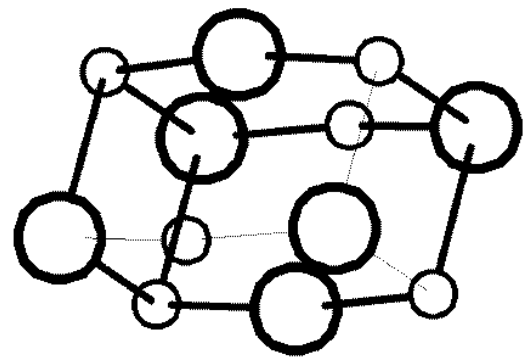
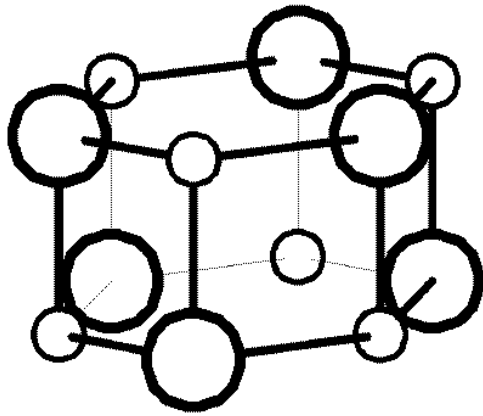
5



0.20

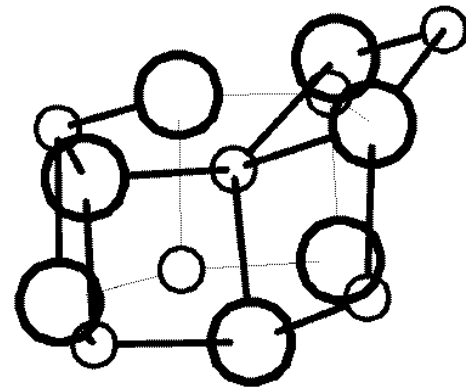
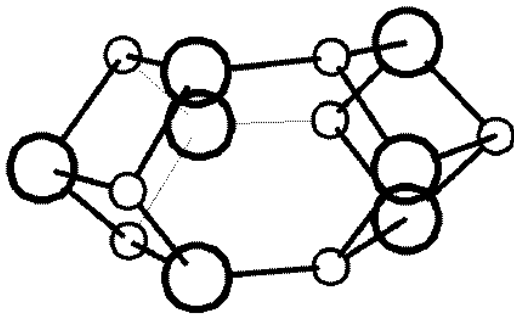
n

6



0.21

7



0.17